0273-2289/96/5902—0187$08.00

Performance of a Magnetically Stabilized Bed Reactor with Immobilized Yeast Cells

V. IVANOVA,*[,1] J. HRISTOV,[2]
E. DOBREVA,[1] Z. AL-HASSAN,[3] AND I. PENCHEV[2]

[1]*Institute of Microbiology, Bulgarian Academy of Sciences, 26 Academician G. Bonchev, 1113 Sofia, Bulgaria;* [2]*Department of Chemical Engineering, Higher Institute of Chemical Technology, Sofia, Bulgaria; and* [3]*Amman State University, Jordan*

Received February 21, 1995; Accepted April 6, 1995

ABSTRACT

This paper is focused on the possibility to apply the magnetic stabilization technique in bioprocessing. The feasibility of a continuous ethanol fermentation process with immobilized *Saccharomyces cerevisiae* cells in a magnetically stabilized bed (MSB) was demonstrated. The fermentation processes were carried out in an external magnetic field, transverse to the fluid flow. The flexibility to change the bed expansion owing to the independent change of the fluid flow and the field intensity (the "magnetization FIRST" mode) permitted the creation of fixed beds with different particle arrangements, which affected the bed porosity, the effective fluid-particle contact area, and the mass transfer processes on the particle-fluid interface. As a result, higher ethanol concentration, ethanol production, and glucose uptake rates than in conventional packed bed reactor were reached.

Index Entries: Magnetically stabilized bed; fluidization; immobilization; *Saccharomyces cerevisiae.*

Abbreviations: dp_{av}, average particle diameter (mm); H, magnetic field intensity (A/m); H_{ms}, minimum field intensity required to create a stabilized bed (A/m); U_{ag}, minimum fluid velocity at which the "homogeneous fluidization of particle aggregates" starts (m/s); U_e, fluid velocity at the onset of the stabilized state in a transverse magnetic

*Author to whom all correspondence and reprint requests should be addressed.

field (m/s); U_{mf}, minimum fluidization velocity (m/s); U_{mfo}, minimum fluidization velocity in absence of a magnetic field (m/s); FIM, fluidizability index in a magnetic field (U_{mf} [in a magnetic field] / U_{mfo}); MSB, magnetically stabilized bed.

INTRODUCTION

Fluidized bed reactors have been successfully employed to carry out multiphase (gas–liquid–solid) reactions in the chemical and biochemical industries. Some of the problems concerning their application were solved by the development of the ferromagnetic particles fluidization (*1–3*) and the bed stabilization by an external magnetic field in continuous chromatographic separation (*4,5*) and continuous cell suspension processing (*6,7*). The main stabilization effects are the increased stability of the interparticle contacts owing to the magnetic cohesive forces and the particles' orientation along the field lines. In the stabilized state, the bed structure is resistant against the destructive action of the flow and the fluid velocity is greater than the minimum fluidization velocity, U_{mfo}, in the absence of a field (*1–3*). The field can be applied in various orientations with respect to the fluid flow. Most of the investigations have been made in an axial field (*1–3,8,9*). The application of a transverse field has been restricted to the area of laboratory scale experiments with electromagnets having iron cores (*10,11*) and the working volume in a homogeneous field in these systems was very small (*8*). Recently, a new possibility to create magnetically stabilized beds (MSB) in a transverse field was proposed (*11,12*). The increase of the working volume was owing to the application of a magnetic system of saddle coils without iron details.

Earlier reports (*13,14*) showed that ferromagnetic beads with immobilized enzymes can be used for reactions accompanied by gas absorption. A magnetic field has been employed to control the movement of immobilized magnetic supports to avoid dowstream processes (*15*) and to govern the bed structure (*13,14*). However, in these studies, the concentrations of the ferromagnetic beads in the working volume were very low, so that the reactors studied differed from these with fixed or fluidized beds in a classical aspect (*16*). It was found that, in the presence of an axial magnetic field (*17*), the biodegradation rate of phenol contaminated water is similar to that in a conventional fixed bed and the throughput of the bed increases significantly.

Limited information is available in the literature regarding cell immobilization on magnetic supports (*14,15,17*). Supports as magnetite distributed in crosslinked polysaccharide beads, magnetite/calcium alginate mixture (*18*), stainless steel spheres, and silica (*19*) have been described. Comments on the supports prepared by different authors have been reported (*19*). These supports have been designed for special goals and limited applicability.

Table 1
Properties of the Magnetic Cores and the Biosupports

Material	Sieve diameter, mm	Density, kg/m³	U_{mfo}, cm/s	dp_{av}, mm
Uncovered particles	0.8–1.0	2800	2.30	0.9
Covered particles	1.0–2.0	1655.2	1.52	1.2

In our previous work (*20*), nonporous supports of magnetite particles covered by zeolite and activated carbon layers were proposed for cell immobilization. The present report continues the studies on the applicability of MSB in the bioprocessing. Our aim is to develop a chemically derivatized biosupport for multiple applications, an important design parameter for large-scale applications of MSB, and to show the effect of the transverse magnetic field on the fluid/particle mass transfer. The glucose conversion to ethanol by immobilized yeasts *Saccharomyces cerevisiae* was used as a model process to demonstrate the applicability of the MSB for continuous bioprocessing.

MATERIALS AND METHODS

Preparation of the Supports

Particles of commercial catalyst "Haldorf Topsoe" KM-1 (Denmark) for ammonia synthesis were used as magnetic cores. They were covered with a stable film of epoxy resin obtained by condensation of epichlorhydrin with bisphenol. One kg of the catalyst (sieve diameter 0.8–1.0 mm) was mixed with 100 g of the epoxy resin and with 9.0 g 1,6-hexanediamine. After 10 min, the magnetic cores were covered with a thin film; then activated carbon powder (Fluka Chemie AG, Buchs, Switzerland, DAB powder, particle size 78% <40 μm, bulk density–495 kg/m³) was added in excess and mixed slowly in a drum for 15 min. During this operation a layer of powder on the resin film was formed. The beads were dried for 48 h at room temperature to complete theresin solidification. The final step was particle washing and drying. The final bead diameter was in the range from 1.0 to 2.0 mm (the average diameter was 1.2 mm). The shape was near spherical. Their properties affecting the fluidization are listed in Table 1. The magnetization at saturation, Ms, of the noncovered particles was determined to be 236.4 kA/m by hysteresiograph (Authomatic DC–BM Curve Tracer, Model BHH-50, Ricken Denshi Co., Japan).

Microorganism and Fermentation Medium

The yeast *S. cerevisiae*, a production strain, was used. The fermentation medium was comprised of g/L: 110–180 g glucose; 2.5 g yeast autolisate; 5

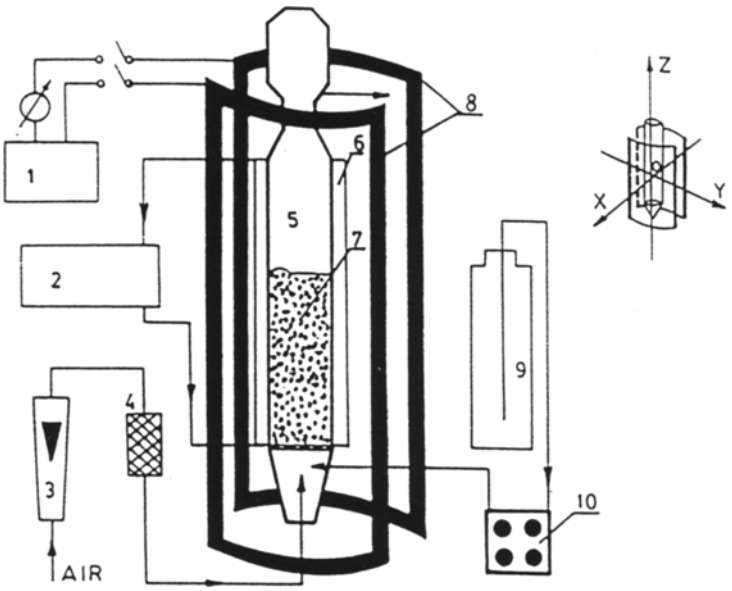

Fig. 1. Fermentor set-up: 1, power supply; 2, thermostat; 3, rotameter; 4, air filter; 5, column; 6, jacket; 7, particle bed; 8, magnetic system (saddle coils); 9, substrate container; 10, peristaltic pump.

g peptone; 3 g KH_2PO_4; 25 mg $CaCl_2$; 3 g $(NH_4)_2SO_4$; 25 mg $MgSO_4$ (heptahydrate); and tap water. All chemicals were from Fluka. The pH was adjusted to 4.5 before sterilization.

Cell Immobilization

The supports were treated consecutively with 1% NaOH and HCl and were washed with distilled water to neutral pH. After sterilization at 105°C, 200 g of the beads were mixed for 3 h at 25°C with 400 mL of cell suspension with yeast cell concentration about 1.1×10^{10} cells/mL. Then glutaraldehyde (Fluka, 32.0 mL of 2.5% solution) was added. After the fixation process (15 min), the particles were washed with abundant quantity of distilled water to remove the excess of cells and glutaraldehyde.

Equipment and Fermentations

Experimental Equipment

The reactor was a jacketed glass column 40 cm in diameter and 80 cm in length with a total reactor volume, including tubings and joints, of 1 L (Fig. 1). A peristaltic pump (model PPIB-05, Poland) was used to supply the liquid. The flowrate was 60.0 mL/h and the dilution rate based on the support volume was 0.37/h. In all experiments, the temperature of the fermentation was maintained at 32°C. The transverse magnetic field was generated by system of two saddle coils (*see* inset in Fig. 1). They had a height of 1.0 m, internal diameter of 0.2 m, and an opening angle of 120°.

The maximum field intensity created was 43 kA/m. The working volume with a homogeneous field distribution had a diameter of 18 cm and a height of 80 cm (the symmetry center coincided with the center of the magnetic system). Its boundaries were determined by measurement of the field distribution by a Hall sonde magnetometer. In this volume, the field nonhomogeneity did not exceed 1% in both the axial and the lateral direction.

There are two operation modes for bed stabilization (*9*): "magnetization FIRST" and "magnetization LAST." In the present study, the "magnetization FIRST" mode was used.

The pressure drop curves and the state diagrams were obtained from experiments without immobilized cells on the bead particles.

Continuous Fermentations

Two modes of operation of the fermentation process were carried out. The first mode was a conventional continuous fermentation in the absence of a magnetic field. The results obtained from this fermentation were used as a basis to detect the magnetic field effect.

The second mode had two steps: The first step was a continuous fermentation in the absence of a magnetic field. After 48 h of cultivation, a magnetic field with intensities of 10–33 kA/m was applied for formation of the stabilized bed. The second step was continuous fermentation in an MSB.

Fermentation Control

The ethanol concentration was measured by gas-chromatography (Erba Science, Model 4300) with a PV 17 fused silica capillary column, 25 m; temperature 35°C; carrier gas—N_2 (2 mL/min); and detector FID. The calculation was done by the method of internal standard: *n*-butanol. The glucose was assayed by the method of Somogyi (*21*). Released cells were measured by the absorbance at 650 nm.

RESULTS

Bed Behavior and Hydrodynamic Conditions

The schematic presentation of the particle arrangement along the field lines in both axial and transverse fields is shown in Fig. 2A and B.

The fluidization behavior of the bed was similar to that observed for noncovered magnetic particles (*22*). However, the use of ferromagnetic cores covered with a nonmagnetic layer required higher field intensities for bed's stabilization owing to the interparticle magnetic force's dependence from the distance between the ferromagnetic cores. The minimum field intensity, H_{ms}, required for bed stabilization was determined using as a criterium the value of the fluidizability index, FIM. The value of 0.85 was used as an indicator for the onset of stabilization. This value of FIM was chosen on the basis of the literature data (*1–3*) and the authors' experience (*11,22*).

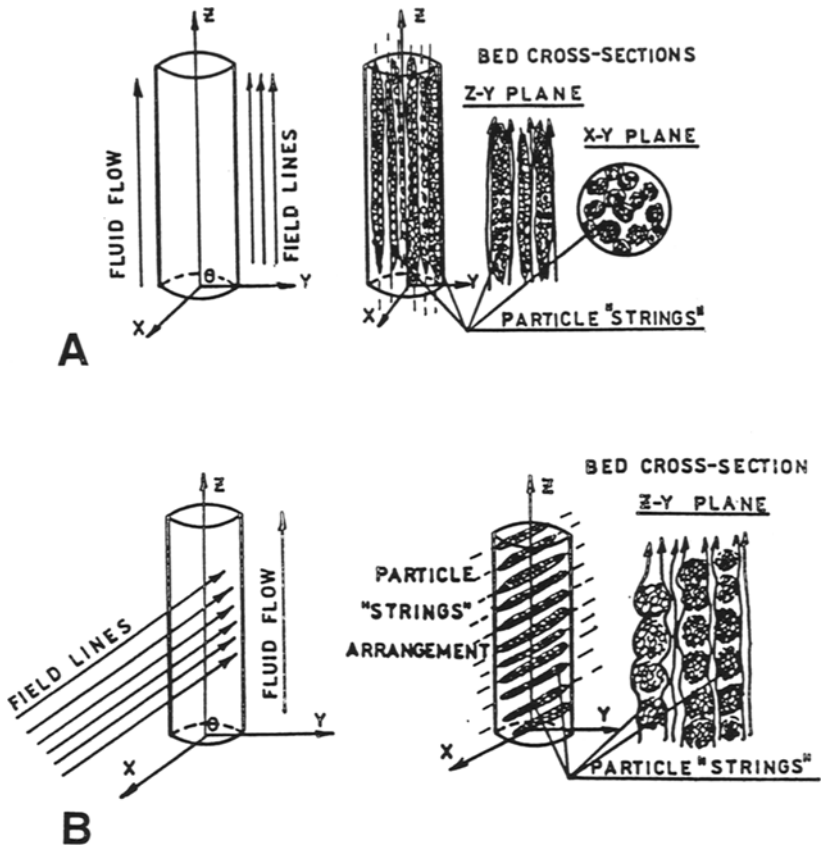

Fig. 2. Fluid flow, field lines, and particles arrangement in stabilized beds by an axial (**A**) and transverse (**B**) magnetic fields.

The boundaries of the stabilized bed are the initial bed expansion point (velocity U_e) and the break-down point (velocity U_{mf}). These critical points can be detected visually and/or from the pressure drop curves for increasing flow. The pressure drop curves for liquid-fluidized beds (noncovered cores) stabilized in transverse fields obtained in these and previous authors' experiments (22) (Fig. 3B) are compared with the results of other authors (9) (Fig. 3A). The experiments in a transverse field indicated that the onset of MSB corresponds to the maximal pressure drop (Fig. 3), whereas the fluidization, i.e., the upper boundary of MSB, coincides with the minimum of the pressure drop curves. In the stabilized state (fixed flowrate), the bed is expanded and fixed with clearly seen particle arrangement along the field lines. The bed expansion is incremental as a result of the incremental increases of the fluid flow.

The hydrodynamic conditions in experiments with noncovered and covered magnetic particles are compared by the state diagrams where the field intensity is an independent parameter that governs the fluidization (Fig. 4). In order to demonstrate the effect of the nonmagnetic layers on

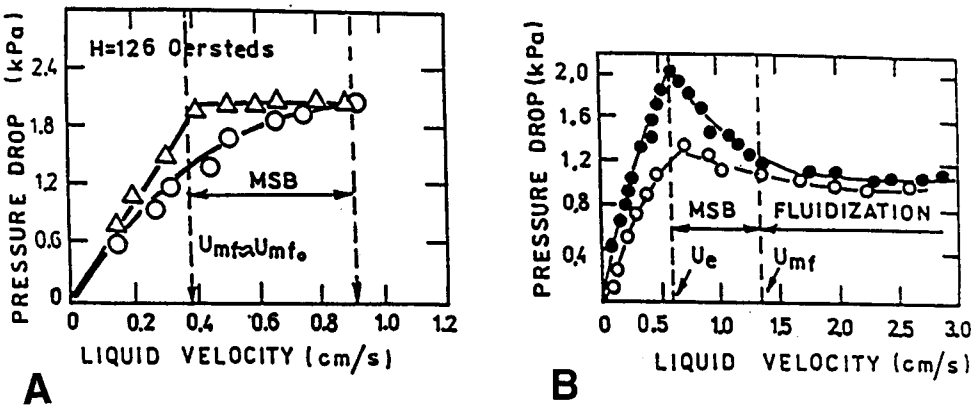

Fig. 3. Pressure drop—liquid velocity curves for increasing flow. (**A**) From Siegel for an axial magnetic field (*9*). △, increasing flow; ○, decreasing flow. (**B**) From these and previous authors experiments (22) for transverse magnetic field. ●, increasing flow, ○, decreasing flow.

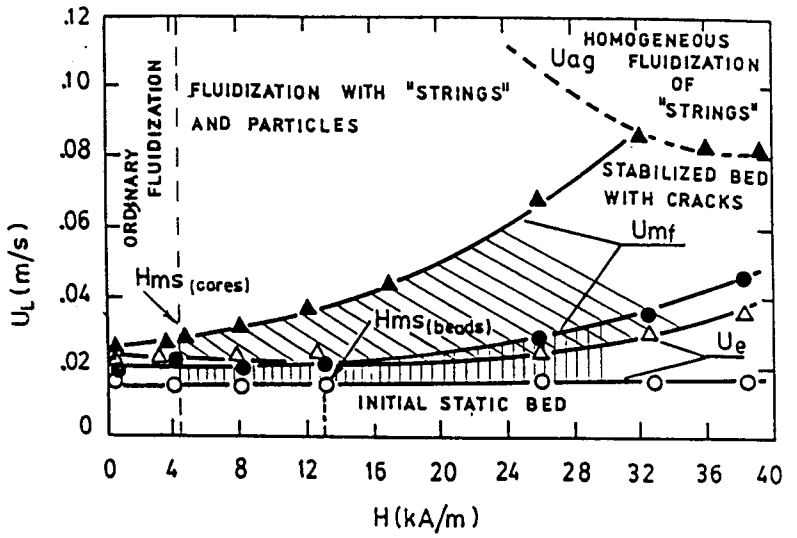

Fig. 4. State diagrams for bed of noncovered and covered particles. Fluidization with water at 20°C and initial bed height of 100 mm. △, U_e of ferromagnetic cores; ○, U_e of carbon covered cores; ▲, U_{mf} of ferromagnetic cores; ●, U_{mf} of carbon covered cores.

the bed stabilization, the velocity ranges in which the stabilized state exists are shown simultaneously in Fig. 4. From the state diagrams, it is clear that the stabilized state bounded by the velocities U_e and U_{mf} decreased with the increase of the thickness of the nonmagnetic layers. Despite this, the stabilization phenomenon permits one to achieve higher fluid velocities with a fixed bed structure. As a result, the cell scouring from the supports at the desired bed expansion and particle arrangement could be eliminated.

Table 2
Continuous Fermentation with Immobilized Yeasts *Saccharomyces cerevisiae* Without a Magnetic Field

Time, h	Residual glucose, g/L		Yield, %		Ethanol, g/L		Ethanol production rate, g/h		Glucose uptake rate, g/h	
	A	B	A	B	A	B	A	B	A	B
24	0.8	73.4	67.4	69.5	37.9	37.9	2.3	2.3	6.6	6.4
48	2.1	77.5	84.0	76.1	47.2	39.8	2.8	2.4	6.5	6.2
72	1.1	75.0	85.9	74.9	48.3	40.2	2.9	2.4	6.5	6.3
120	1.9	77.6	88.6	76.0	49.8	39.8	3.0	2.4	6.5	6.2
240	3.5	83.0	81.5	75.6	45.8	37.5	2.8	2.2	6.4	5.8
288	3.9	86.0	74.7	74.9	42.0	36.0	2.5	2.2	6.4	5.7

A, inlet glucose concentration 110.0 g/L; B, inlet glucose concentration 180.0 g/L.

The bed behavior here could be determined as a lying between the liquid-solid (*9*) and the liquid-gas-solid (*12,23,24*) MSBs, owing to the gas-phase consisting of CO_2 produced *in situ*. However, the amount of CO_2 produced in the fermentation experiments was enough to assure the substrate mixing (*25*), but the magnetic field suppressed the bubble coalescence. The bubble sizes observed in the experiments did not exceed the pore diameter in the packed beds, so they were considered as liquid-solid stabilized beds approximately and also the cell scouring from the supports was diminished.

Fermentations without Application of Magnetic Field

The results from these fermentation experiments are summarized in Table 2. At low, but optimal substrate concentration (*25*), (Table 2A), the glucose was completely fermented to ethanol and cell material. The ethanol concentration was in the range of 47.0–50.0 g/L, which represented about 88% of the theoretical yield. The immobilized yeasts utilized the substrate with a glucose uptake rate in the range of 6.6–6.4 g/h and the ethanol production rate was approx. 3.0 g/h. After 240 h of continuous fermentation, the ethanol yield and the other fermentation parameters began to decrease. These results could be attributed to both the product inhibition and strain characteristics. The cell concentration in the medium reached the value of 2.0×10^7 cells/mL (the daughter cells could not be retained on the supports) and then also began to decrease. This cell concentration was about 100 times lower than the biomass concentration in batch ethanol fermentation with free yeast cells (1.5×10^9 cells/mL, [*25*]).

In order to compare the immobilized yeast behavior at higher substrate concentrations, a series of experiments were carried out at the same experimental conditions, but at 180.0 g/L glucose concentration in the

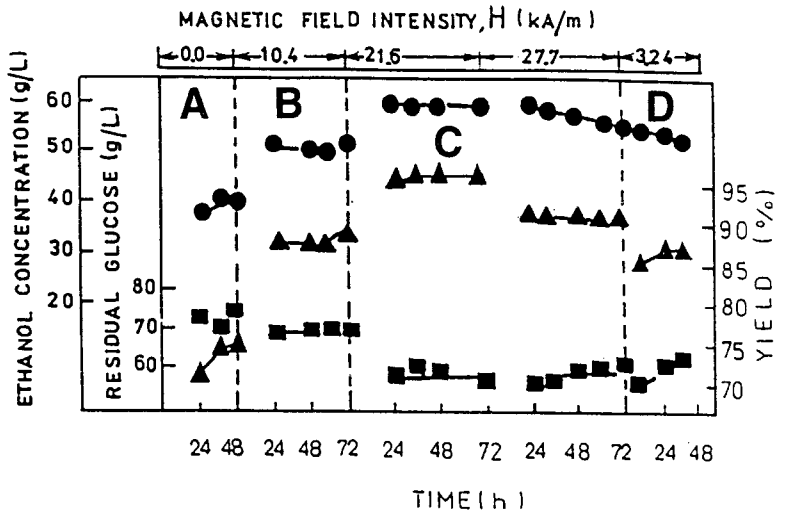

Fig. 5. Fermentation process with immobilized yeasts *Saccharomyces cerevisiae* as a function of the magnetic field intensity. The time is presented in h from the creation of the stabilized bed. ●, ethanol concentration; ▲, yield; ■, residual glucose concentration.

Table 3
Effect of the Field Intensity on Some Fermentation Parameters (averaged results)

Field, kA/m	Bed height, m	Residual glucose, g/L	Yield, %	Ethanol production rate, g/h	Glucose uptake rate, g/h
0	0.130	78.8	74.8	2.3	6.0
10.4	0.135	69.7	87.4	3.0	6.6
21.6	0.145	59.6	95.8	3.5	7.2
27.7	0.155	58.1	92.2	3.4	7.3
32.4	0.170	59.5	87.7	3.2	7.3

medium. It can be seen (Table 2B) that, at these conditions, all fermentation parameters (ethanol concentrations, yield, productivity, ethanol production, and glucose uptake rates) were lower. The strain utilized a lower quantity of glucose than in the aforementioned process. This fact can be explained by substrate inhibition. Despite this, these fermentation conditions were used in the next experiments in magnetically stabilized bed, because the substrate was consumed completely at the optimal fermentation conditions and any changes in the immobilized yeast behavior owing to the magnetic field application could not have been detected.

Fermentation in a Magnetically Stabilized Bed

The results are summarized in Fig. 5 as a function of the field intensity, and also in Table 3.

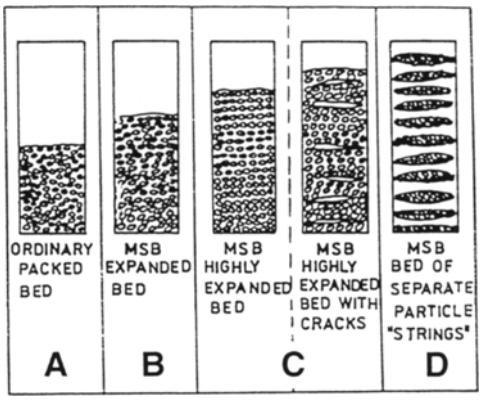

Fig. 6. Schematic presentation of the particle arrangement in the bed as a function of the field intensity (A, B, C, and D are discussed in the text).

During the first 48 h, the fermentation was carried out without a magnetic field. After that, the magnetic field was applied to the initial fixed bed and then the liquid flow rate was adjusted to obtain the desired expansion. After that the liquid flow was decreased slowly to 60 mL/h. Under these conditions, the process was carried out 72 h. This procedure was performed several times at various field intensities.

From the experimental results, it can be seen that the bed status (i.e., field intensities, bed height, and the particle arrangement) had a significant effect on both the glucose uptake rate and the ethanol production rate. Both increased parallel to the increase of the field intensity. This increase was about 1.5 times for the ethanol production rate and about 115% for the glucose uptake rate. The ethanol concentration reached 59.0 g/L at a 96% yield of the theoretical. The productivity was 21.8 g/L h and the residual glucose concentration decreased to 55–60 g/L compared to 75–85 g/L in the packed bed fermentation. These positive results were obtained at all the field intensities applied, but the magnetic field effects were more clearly demonstrated at field intensities from 10.4 up to 27.7 kA/m. At higher field intensities, the released biomass increased from 1.0 to 1.5 $\times$ 10^7 cells/mL; the ethanol concentration was lower and the fermentation process effectiveness began to decrease.

DISCUSSION

According to the bed internal structure (Fig. 6), the results from Table 3 and Fig. 5, and from the viewpoint that the bed has different internal structure at different field intensities, it was possible to divide the process into several zones and to explain the fermentation results:

1. Zone A. The field was not applied, the particle arrangement and the fermentation effectiveness were similar to that in conventional packed beds.

2. Zone B. The field intensity was low. The magnetic forces were enough to orient the particle arrangement parallel to the field lines. As a result, the bed expansion was not significant, but the increase of the bed porosity increased the glucose consumption and the ethanol yield.
3. Zone C. The interparticle magnetic forces increased and led to a significant bed expansion. However, they were not strong enough and the formation of particle aggregates ("strings") and cracks in the bed was impossible. As a result, the maximum particle-fluid contact area and the maximal effect on the fermentation process (higher ethanol concentration and production rate, higher product yield) were obtained. This fact can be attributed to the effect of particle arrangement on the effective fluid-particle contact area. From zone A up to zone C, the particle arrangement along the field lines led to an increasing bed porosity. The latter affected the mass transfer processes on the particle-fluid interface.
4. Zone D. The field intensity was high and the bed structure was anisotropic. The bed consisted of particle "strings" oriented along the field lines and divided by channels or cracks, which decreased the efficiency of the fermentation. The effective contact area between the fluid and particle surfaces decreased owing to the particle aggregation into "strings." In this case, the effective fluid-particle contacts were on the aggregates' surfaces. On these surfaces, the convective hydrodynamic effects on the mass transfer processes were significant owing to the greater fluid velocities in the voids between them. However, in the bulk of the aggregates, the diffusion dominated over the convective transport, which decreased the efficiency of the particle-fluid transfer processes. This comment is supported by the fact that the glucose consumption and the ethanol production decreased.

It can be mentioned that, in the fermentation process reported in this study, the released cell concentration in the absence of a magnetic field or at lower field intensities was lower than that in conventional batch ethanol fermentation or in packed-bed fermentation with immobilized in Ca-alginate yeast cells (*25*). This result can be explained by the fact that the fermentation was carried out in a fixed bed (the stabilized bed has a fixed structure) and the growth of CO_2 bubbles was supressed, which prevented the scouring of the cells from the supports.

CONCLUSIONS

A magnetically stabilized bed created in a transverse magnetic field can be used in fermentations with immobilized yeast cells. The results of

this study demonstrated the applicability of the magnetic carbon supports in long-term fermentation. They could be arranged in different fixed structures stabilized by a transverse magnetic field. The application of the MSB in the process of glucose fermentation to ethanol increased the ethanol production and the glucose uptake rates.

REFERENCES

1. Filippov, M. V. (1960), *Troudii Inst. Fiz. Latv. SSR* **12,** 215–236.
2. Rosensweig, R. E. (1979), *Science* **204,** 57–64.
3. Siegel, J. H. (1988), *Chem. Eng. Comm.* **67,** 43–54.
4. Burns, M. A. and Graves, D. J. (1985), *Biotechnol. Progress* **1,** 45–50.
5. Burns, M. A. and Graves, D. J. (1987), *Reactive Polymers* **6,** 45–50.
6. Terranova, B. E. and Burns, M. A. (1989), *Biotechnol. Progress* **5,** 98–104.
7. Terranova, B. E. and Burns, M. A. (1991), *Biotechnol. Bioeng.* **37,** 110–120.
8. Liu, Y. A., Hamby, R. K., and Colberg, R. D. (1991), *Powder Technol.* **64,** 3–41.
9. Siegel, J. H. (1987), *Powder Technol.* **52,** 139–148.
10. Burns, M. A. and Graves, D. J. (1988), *Chem. Eng. Commun.* **67,** 315–319.
11. Penchev, I. and Hristov, J. (1990), *Powder Technol.* **62,** 1–11.
12. Penchev, I., Al-Hassan, Z., and Hristov, J. (1991), in *La fluidization—Recents Progres en Genie des Procedes,* vol. 5, Laguerie, C. and Guidon, P., eds., Lavoisie, Paris, pp. 341–351.
13. Sada, S., Katoh, S., Shiozawa, M., and Fukui, T. (1981), *Biotechnol. Bioeng.* **23,** 2561–2567.
14. Sada, S., Katoh, S., Shiozawa, M., and Matsui, I. (1983), *Biotechnol. Bioeng.* **25,** 2285–2292.
15. Sada, S., Katoh, S., Shiozawa, M., and Matsui, I. (1981), *J. Chem. Eng. Japan* **14,** 496,497.
16. Kunii, D. and Levenspiel, O. (1991), *Fluidization Engineering,* 2nd ed., Butterworths-Heineman, Boston.
17. Hu, T. T. and Wu, J. K. (1987), *Chem. Eng. Res. Des.* **65,** 238–242.
18. Burns, M. A., Kvesitadze, G. I., and Graves, D. J. (1985), *Biotechnol. Bioeng.* **27,** 137–145.
19. Goetz, V., Remaund, M., and Graves, D. J. (1991), *Biotechnol. Bioeng.* **37,** 614–626.
20. Al-Hassan, Z., Ivanova, V., Dobreva, E., Penchev, I., Hristov, J., Rachev, R., and Petrov, R. (1991), *J. Ferment. Bioeng.* **71.**
21. Somogyi, M. (1952), *J. Biol. Chem.* **196,** 19–23.
22. Penchev, I. and Hristov, J. (1990), in *Fluidization and Fluid/Particle Systems,* Casal, J. and Arnaldos, J., eds., Univ. Politechnica of Catalunya, Barcelona, Spain, pp. 173–180.
23. Kwauk, M., Ma, X., Ouyang, F., Wu, Y., Weng, D., and Cheng, L. (1992), *Chem. Eng. Sci.* **47,** 3467–3474.
24. Fan, L. S. (1989), *Gas-Liquid-Solid Fluidization Engineering,* Butterworths-Heineman, Boston.
25. Rychtera, M., Basarova, G., and Ivanova, V. (1987), in *4th European Congress on Biotechnology,* vol. 2, Neijssel, O. M., Van der Meer, R. R., and Luvben, K., eds., Elsevier, Amsterdam, pp. 107–110.